



Edge detection based on Krawtchouk polynomials



Daniel Rivero-Castillo^a, Héctor Pijeira^{b,*}, Pedro Assunção^c

^a Universidad Politécnica de Madrid, Spain

^b Universidad Carlos III de Madrid, Spain

^c Instituto de Telecomunicações and Polytechnic Institute of Leiria-ESTG, Portugal

ARTICLE INFO

Article history:

Received 31 July 2014

Received in revised form 12 November 2014

MSC:

94A08

94A11

33C45

33C47

42C05

Keywords:

Image processing

Edge detection

Krawtchouk polynomials

Discrete orthogonal polynomials

ABSTRACT

Discrete orthogonal polynomials are useful tools in digital image processing to extract visual object contours in different application contexts. This paper proposes an alternative method that extends beyond classic first-order differential operators, by using the properties of Krawtchouk orthogonal polynomials to achieve a first order differential operator. Therefore, smoothing of the image with a 2-D Gaussian filter is not necessary to regularize the ill-posed nature of differentiation. Experimentally, we provide simulation results which show that the proposed method achieves good performance in comparison with commonly used algorithms.

© 2015 Elsevier B.V. All rights reserved.

1. Introduction

Edge detection plays a relevant role in digital image processing algorithms for many different fields of application. From computer vision applications in the industry and medical fields [1] to 3D video and image coding [2], visual object contour detection is one of the functions based on edge detection, which is very often required as part of more complex operations. For instance, image segmentation for visual object identification and recognition, definition of regions of interest within a visual scene for selective coding, inspection or attention-based processing, all require fast and efficient edge detection algorithms [3].

There are various methods for edge detection in digital images based on a fairly consolidated theory (cf. [4, Chapter 15] and [5, Sections 4.5–4.6]). Most of the edge extraction techniques operate a predefined format of digital image representation (e.g. RGB, gray-scale, etc.) using differential operators to find relevant transitions in the image intensity. Such transitions represent edges, which are defined as the borders of either visual objects or image regions, also establishing the boundaries between overlapping objects or different regions.

In many applications the relevant region boundaries, i.e., edges, are found on the luminance component of images, which require a gray-scale representation, even though other formats might be used (e.g. RGB). Since the majority of important low-level feature related information exists in gray-scale images, such as edges, smooth regions, and textures, in this work we

* Corresponding author.

E-mail addresses: daniel.rivero@upm.es (D. Rivero-Castillo), hpijeira@math.uc3m.es (H. Pijeira), amado@co.it.pt (P. Assunção).

only consider gray-scale representation images. The method for edge detection in gray-scale images proposed in this paper is based on approximate the derivatives of the function image using the Krawtchouk orthogonal polynomials properties.

The structure of this paper is as follows. In the next section we present the theoretical framework of the paper and the basic properties of the Krawtchouk polynomials in one variable. In Section 3 we establish the Krawtchouk polynomials in two variables, which are used to approximate the image in the sense of least squares. In Section 4 we explain how we analyze the image by blocks and for the numerical experiments we consider a particular cases to obtain close formulas. In Section 5, we describe our algorithm of edge detection based on the Krawtchouk polynomials. Finally in the last section we present experimental results and concluding remarks of this work.

2. Krawtchouk polynomials in one variable

This work relies on well known references often cited to establish the basic theory of orthogonal polynomials which are [6,7]. However these monographs essentially deal with orthogonal polynomials with respect to a continuous inner product whilst for the purpose of our work we are focused on the discrete case as required by the type of data we are dealing with, i.e., digital images. On the theory discrete orthogonal polynomials and applications we suggest the Refs. [8,9] or [10, Chapter 5].

Let $N \in \mathbb{N}$, $\Lambda := \{x_0, x_1, \dots, x_N\} \subset \mathbb{R}$, where $x_0 < x_1 < \dots < x_N$, $\mathbf{F}(\Lambda)$ be the set of all real functions on Λ , \mathbb{P} be the set of all real coefficient polynomials and $\mathbb{P}_N \subset \mathbb{P}$ be the set of polynomials of degree at most N . Note that any real function of a discrete variable $f \in \mathbf{F}(\Lambda)$ can be seen as the restriction on Λ of a number of functions of real variable, in particular the Lagrange interpolation polynomial $P \in \mathbb{P}_N$ such that $P(x_i) = f(x_i)$ for $i = 0, 1, \dots, N$. Then we have a natural identification between the sets $\mathbf{F}(\Lambda)$ and \mathbb{P}_N .

We call *weight function* (or simply *weight*) to any positive function μ on Λ and we say that it is *normalized* when $\sum_{k=0}^N \mu(x_k) = 1$.

Let the pair (Λ, μ) , where μ is a weight defined on Λ . The inner product on \mathbb{P}_N associated to (Λ, μ) is defined by:

$$\langle f, g \rangle_{\Lambda, \mu} = \sum_{k=0}^N f(x_k)g(x_k)\mu(x_k), \quad f, g \in \mathbb{P}_N \tag{1}$$

with a corresponding norm $\|f\|_{\Lambda, \mu} = \sqrt{\langle f, f \rangle_{\Lambda, \mu}}$.

A family of polynomials $\{p_k\}_{k=0}^m$ with $m \leq N$ is *orthogonal* with respect to the inner product (1) if p_k is a polynomial of degree k with positive leading coefficient and

$$\langle p_n, p_m \rangle_{\Lambda, \mu} = \begin{cases} \neq 0 & \text{if } n = m, \\ = 0 & \text{if } n \neq m. \end{cases} \tag{2}$$

If $\|p_k\|_{\Lambda, \mu} = 1$ for all $0 \leq k \leq N$, the family $\{p_k(x)\}_{k=0}^m$ is called *orthonormal* with respect to (1). Finally if for all $0 \leq k \leq N$ the leading coefficient of $p_k(x)$ is equal to one, then $\{p_k(x)\}_{k=0}^m$ is called a family of *monic* orthogonal polynomials with respect to (1).

Note that (2) is equivalent to the condition

$$\langle p_n, x^j \rangle_{\Lambda, \mu} = \sum_{k=0}^N p_n(x_k)x_k^j \mu_k = 0, \quad \text{for } j = 0, 1, \dots, n. \tag{3}$$

Then given a weight function μ , the relations (3) form a system of $N + 1$ unknowns (the coefficients of polynomial), which determine the orthogonal polynomial $p_n(x)$ except for a multiplicative constant which may depend on n .

In this paper we find a new form to obtain approximations to the derivatives in each point of the image making use of a family of discrete orthogonal polynomials called Krawtchouk polynomials, that are orthogonal with respect to the binomial distribution (cf. [10, Section 5.4]). In the remainder of the section, we state some definitions and properties about the monic Krawtchouk polynomials in one variable.

Definition 2.1. Let $N \in \mathbb{N}$, $\Lambda_N = \{0, 1, 2, \dots, N\}$, $\alpha \in]-1, 1[$ and $w_{N,\alpha}(x)$ the weight function

$$w_{N,\alpha}(x) = \binom{N}{x} \alpha^x (1 - \alpha)^{N-x}, \quad \text{for all } x \in \Lambda_N. \tag{4}$$

We say that $\kappa_n^\alpha(x, N) = x^n + \dots$, with $n \leq N$, is the *nth monic Krawtchouk polynomial* with respect to the pair $(\Lambda_N, w_{N,\alpha})$ if

$$\langle \kappa_n^\alpha(\cdot, N), x^j \rangle_{N,\alpha} = \sum_{i=0}^N \kappa_n^\alpha(i, N) x^j w_{N,\alpha}(i) = 0,$$

for all $j = 0, 1, \dots, N$, where $\langle \cdot, \cdot \rangle_{N,\alpha} = \langle \cdot, \cdot \rangle_{\Lambda_N, w_{N,\alpha}}$.

Obviously, from the binomial theorem, the weight function (4) is normalized. The n th monic Krawtchouk polynomial in one variable can be generated by the formula (cf. [10, (5.4.3)])

$$\kappa_n^\alpha(x, N) = \sum_{j=0}^n \binom{n}{j} \alpha^{n-j} (1 - \alpha)^j (x - N)_{n-j} (x - j + 1)_j, \tag{5}$$

where $(a)_j$ denotes the Pochhammer symbol or shifted factorial as in [10, (1.1.8)].

From [10, (5.2.8)], we obtain the norms of the n th polynomials (5)

$$\|\kappa_n^\alpha(\cdot, N)\|_{N,\alpha}^2 = \sum_{i=0}^N (\kappa_n^\alpha(i, N))^2 w_{N,\alpha}(i) = \binom{N}{n} n!^2 (\alpha - \alpha^2)^n.$$

If f is a function of one variable, we define the differences of first order as $\Delta_+ f(x) = f(x + 1) - f(x)$, $\Delta f(x) = \frac{1}{2}(f(x + 1) - f(x - 1))$, where the differences Δf of first order is the usual central-difference formulas on 2 nodes (cf. [11, Table 6.3]). For a function in two variables \mathbf{f} we define the partial differences of first order as:

$$\Delta_x \mathbf{f}(x, y) = \frac{\mathbf{f}(x + 1, y) - \mathbf{f}(x - 1, y)}{2}, \quad \Delta_y \mathbf{f}(x, y) = \frac{\mathbf{f}(x, y + 1) - \mathbf{f}(x, y - 1)}{2}. \tag{6}$$

Most of the results contained in this paper can be obtained analogously for other families of discrete orthogonal polynomials (see [10, Chapter 5]). However, we use the Krawtchouk polynomials because they allow to obtain closed expressions for the discrete derivatives (differences) of the polynomials in one and two variables. The next proposition is straightforward from the basic properties of Krawtchouk polynomials in [10, Section 5.4] and includes some of the aforementioned closed expressions.

Proposition 2.1. *The monic Krawtchouk polynomial, with $\alpha \in] - 1, 1[$, satisfies the following relations:*

$$\Delta_+ \kappa_n^\alpha(x, N) = n \kappa_{n-1}^\alpha(x, N - 1). \tag{7}$$

$$\Delta \kappa_n^\alpha(x, N) = \frac{n}{2} (\kappa_{n-1}^\alpha(x, N - 1) + \kappa_{n-1}^\alpha(x - 1, N - 1)) \tag{8}$$

Proof. From [10, (5.4.4)], we get the relations (7) for the forward difference. The central difference $\Delta \kappa_n^\alpha(x, N)$ in (8), is a direct consequences of (7). \square

3. Krawtchouk polynomials in two variables

A gray-scale image with resolution $(N_1 + 1) \times (N_2 + 1)$ pixels ($N_1, N_2 \in \mathbb{N}$) can be considered as a function of two variables $\mathbf{I}(x, y)$ defined on the set $\Lambda_{N_1} \times \Lambda_{N_2}$, where $\Lambda_{N_1} = \{0, 1, \dots, N_1\}$ and $\Lambda_{N_2} = \{0, 1, \dots, N_2\}$, i.e.

$$\begin{aligned} \mathbf{I} : \Lambda_{N_1} \times \Lambda_{N_2} &\longrightarrow [0, 1], \\ (x, y) &\longrightarrow \mathbf{I}(x, y). \end{aligned}$$

Hence, the values of \mathbf{I} on $\Lambda_{N_1} \times \Lambda_{N_2}$ can be represented by the matrix \mathcal{I} of order $(N_1 + 1) \times (N_2 + 1)$

$$\mathcal{I} = \begin{bmatrix} \mathbf{I}(0, 0) & \mathbf{I}(0, 1) & \cdots & \mathbf{I}(0, N_2) \\ \mathbf{I}(1, 0) & \mathbf{I}(1, 1) & \cdots & \mathbf{I}(1, N_2) \\ \vdots & \vdots & \ddots & \vdots \\ \mathbf{I}(N_1, 0) & \mathbf{I}(N_1, 1) & \cdots & \mathbf{I}(N_1, N_2) \end{bmatrix}. \tag{9}$$

Let \mathbb{P}_{N_1, N_2} be the linear space of polynomials in the variables x and y , of degree at most N_1 and N_2 respectively.

To study an image as a polynomial in two variables, we need to introduce the Krawtchouk polynomials in two variables or bivariate Krawtchouk polynomials.

Definition 3.1. Let $N_1, N_2 \in \mathbb{N}$, $\alpha_1, \alpha_2 \in]0, 1[$, $\Lambda_{N_1} = \{0, \dots, N_1\}$ and $\Lambda_{N_2} = \{0, \dots, N_2\}$. We call *Two-dimensional Krawtchouk polynomials* or *2D monic Krawtchouk polynomials* to the polynomial in two variables $\mathbf{K}_{n,m}^{\alpha_1, \alpha_2}(x, y) = \kappa_n^{\alpha_1}(x, N_1) \kappa_m^{\alpha_2}(y, N_2)$, where $(x, y) \in \Lambda_{N_1} \times \Lambda_{N_2}$.

Note that the set of 2D monic Krawtchouk polynomials

$$\{\mathbf{K}_{n,m}^{\alpha_1, \alpha_2}\} = \{\kappa_n^{\alpha_1}(\cdot, N_1)\} \otimes \{\kappa_m^{\alpha_2}(\cdot, N_2)\},$$

where the symbol \otimes denotes the tensor product of the set of polynomials $\{\kappa_n^{\alpha_1}(\cdot, N_1)\}$ and $\{\kappa_m^{\alpha_2}(\cdot, N_2)\}$ as in [12, Section 12-3]. The 2D monic Krawtchouk polynomials are orthogonal with respect to the next inner product on \mathbb{P}_{N_1, N_2}

$$\langle \mathbf{f}, \mathbf{g} \rangle_{2D} = \sum_{i=0}^{N_1} \sum_{j=0}^{N_2} \mathbf{f}(x_i, x_j) \mathbf{g}(x_i, x_j) w_{N_1, \alpha_1}(x_i) w_{N_2, \alpha_2}(x_j). \tag{10}$$

(see [12, Lemma 12-1]), furthermore

$$\begin{aligned} \langle \mathbf{K}_{n,m}^{\alpha_1, \alpha_2}, \mathbf{K}_{r,s}^{\alpha_1, \alpha_2} \rangle_{2D} &= \langle \kappa_n^{\alpha_1}, \kappa_r^{\alpha_1} \rangle_{N_1, \alpha_1} \langle \kappa_m^{\alpha_2}, \kappa_s^{\alpha_2} \rangle_{N_2, \alpha_2} \\ &= \begin{cases} 0 & |n - r| + |m - s| > 0, \\ \|\mathbf{K}_{n,m}^{\alpha_1, \alpha_2}\|_{2D}^2 > 0 & |n - r| + |m - s| = 0, \end{cases} \end{aligned}$$

where $\|\mathbf{f}\|_{2D} = \sqrt{\langle \mathbf{f}, \mathbf{f} \rangle_{2D}}$.

For the 2D monic Krawtchouk polynomials we have the next finite difference formulas:

$$\begin{aligned} \Delta_x \mathbf{K}_{n,m}^{\alpha_1, \alpha_2}(x, y) &= (\Delta_x \kappa_n^{\alpha_1}(x, N_1)) \kappa_m^{\alpha_2}(y, N_2). \\ \Delta_y \mathbf{K}_{n,m}^{\alpha_1, \alpha_2}(x, y) &= (\Delta_y \kappa_m^{\alpha_2}(y, N_2)) \kappa_n^{\alpha_1}(x, N_1). \end{aligned} \tag{11}$$

From the standard theory of approximation of functions (cf. [12, Chapter 12]), for $M_1 \in \Lambda_{N_1} \setminus \{0\}$ and $M_2 \in \Lambda_{N_2} \setminus \{0\}$, the polynomial of total degree $(M_1 - 1) \times (M_2 - 1)$

$$\mathbf{P}_{M_1, M_2}(x, y) = \sum_{n=0}^{M_1-1} \sum_{m=0}^{M_2-1} \beta_{n,m} \mathbf{K}_{n,m}^{\alpha_1, \alpha_2}(x, y), \quad \text{where } \beta_{n,m} = \frac{\langle \mathbf{I}, \mathbf{K}_{n,m}^{\alpha_1, \alpha_2} \rangle_{2D}}{\langle \mathbf{K}_{n,m}^{\alpha_1, \alpha_2}, \mathbf{K}_{n,m}^{\alpha_1, \alpha_2} \rangle_{2D}} \tag{12}$$

is such that $\min_{\mathbf{Q} \in \mathbb{P}_{M_1, M_2}} \|\mathbf{I} - \mathbf{Q}\|_{2D} = \|\mathbf{I} - \mathbf{P}_{M_1, M_2}\|_{2D}$, i.e. \mathbf{P}_{M_1, M_2} is the polynomial of least square approximation of \mathbf{I} in \mathbb{P}_{M_1, M_2} and we write $\mathbf{I}(x, y) \approx \mathbf{P}_{M_1, M_2}(x, y)$. Furthermore, if $M_1 = N_1 + 1$ and $M_2 = N_2 + 1$, then $\mathbf{I} = \mathbf{P}_{N_1, N_2}$.

4. Computation of the discrete derivative by blocks

In order to detect the edges points, we analyze the entire image \mathcal{I} , by blocks $\mathcal{I}_{i,j}$ of fixed-size $(n_1 + 1) \times (n_2 + 1)$, where $n_1 < N_1$ and $n_2 < N_2$. We recall that the blocks are all of the same size.

First, let us introduce some notations and definitions. If $\mathcal{A} = [a_{ij}]$ is a $u \times v$ real matrix, then \mathcal{A}^T denotes the transpose matrix and $\text{vec}(\mathcal{A})$ is the column vector of (uv) entries defined as $\text{vec}(\mathcal{A}) = (a_{11}, \dots, a_{u1}, a_{12}, \dots, a_{u2}, \dots, a_{1v}, \dots, a_{uv})^T$. Let $\bar{\mathbf{a}}_n = (\mathbf{a}_n(0), \dots, \mathbf{a}_n(n_1))$ and $\bar{\mathbf{b}}_m = (\mathbf{b}_m(0), \dots, \mathbf{b}_m(n_2))$ be two row vectors of order $(n_1 + 1)$ and $(n_2 + 1)$ respectively, where

$$\mathbf{a}_n(v) = \frac{\kappa_n^{\alpha_1}(v, n_1) w_{n_1, \alpha_1}(v)}{\|\kappa_n^{\alpha_1}\|_{n_1, \alpha_1}^2}, \quad \mathbf{b}_m(v) = \frac{\kappa_m^{\alpha_2}(v, n_2) w_{n_2, \alpha_2}(v)}{\|\kappa_m^{\alpha_2}\|_{n_2, \alpha_2}^2}.$$

The matrix $\mathcal{C}_{n_1, n_2}(n, m) = \bar{\mathbf{a}}_n^T \bar{\mathbf{b}}_m$ is of order $(n_1 + 1) \times (n_2 + 1)$ and only depends on the size of the blocks, but not of its entries.

Let $\beta_{n,m}(i, j)$ be the coefficient given by (12), considering $\mathcal{I} = \mathcal{I}_{i,j}$. This coefficient can be computed as follows:

$$\beta_{n,m}(i, j) = \langle \text{vec}(\mathcal{I}_{i,j}), \text{vec}(\mathcal{C}_{n_1, n_2}(n, m)) \rangle_2, \tag{13}$$

where $\langle \cdot, \cdot \rangle_2$ is the usual Euclidean inner product on $\mathbb{R}^{(n_1+1)(n_2+1)}$.

Let $\mathcal{B}_{n,m}$ be the matrix of all coefficients $\beta_{n,m}(i, j)$, with $i = 0, \dots, n_1$ and $j = 0, \dots, n_2$. From (13), $\mathcal{B}_{n,m} = \mathcal{I} * \mathcal{C}_{n_1, n_2}(n, m)$, where the symbol $*$ indicates the 2-D discrete convolution of matrices (cf. [13, Section 15.1.4]). Using the discrete Fourier transform, the convolution of these matrices can be optimized, improving significantly the CPU time (cf. [13, Chapter 15]).

For each pixel (i, j) of the image \mathcal{I} , we compute the discrete partial derivative (6) of the approximation (12), only considering the information contained in the “neighborhood” $\mathcal{I}_{i,j}$. When this process is finished, we obtain two matrices \mathcal{P}_x and \mathcal{P}_y of the same size of \mathcal{I} , where each entry (i, j) is the partial derivatives with respect to x or y . In the next section, these matrices allow us to have a good estimate of the modulus of gradient on each point (i, j) of \mathcal{I} .

In order to make numerical experiments we consider the parameters of Krawtchouk polynomials $\alpha_1 = \alpha_2 = \alpha = \frac{1}{2}$, and $n_1 = n_2 = n_t = 4$, i.e. we approximate the calculus of the discrete derivatives considering the information of the block

$\mathcal{I}_{i,j}$ of order 5×5 , with center on the entry $\mathbf{I}(i, j)$:

$$\mathcal{I}_{i,j} = \begin{bmatrix} \mathbf{I}(i-2, j-2) & \mathbf{I}(i-2, j-1) & \mathbf{I}(i-2, j) & \mathbf{I}(i-2, j+1) & \mathbf{I}(i-2, j+2) \\ \mathbf{I}(i-1, j-2) & \mathbf{I}(i-1, j-1) & \mathbf{I}(i-1, j) & \mathbf{I}(i-1, j+1) & \mathbf{I}(i-1, j+2) \\ \mathbf{I}(i, j-2) & \mathbf{I}(i, j-1) & \mathbf{I}(i, j) & \mathbf{I}(i, j+1) & \mathbf{I}(i, j+2) \\ \mathbf{I}(i+1, j-2) & \mathbf{I}(i+1, j-1) & \mathbf{I}(i+1, j) & \mathbf{I}(i+1, j+1) & \mathbf{I}(i+1, j+2) \\ \mathbf{I}(i+2, j-2) & \mathbf{I}(i+2, j-1) & \mathbf{I}(i+2, j) & \mathbf{I}(i+2, j+1) & \mathbf{I}(i+2, j+2) \end{bmatrix}.$$

From (12) with $M_1 = M_2 = M_t$, we have for $i = 0, \dots, N_1$ and $j = 0, \dots, N_2$ the polynomial block approximation:

$$\mathbf{P}_{M_t, M_t}^{(i,j)}(x, y) \approx \mathbf{I}(i+x-2, j+y-2), \quad (x, y) \in \Lambda_{n_t} \times \Lambda_{n_t}, \tag{14}$$

where for each fixed point (i, j) the polynomial $\mathbf{P}_{M_t, M_t}^{(i,j)}(x, y)$ is given by (12), and the coefficients $\beta_{n,m}(i, j)$ by (13).

Now taking into account the fact that for $x = y = 2$ in the approximation (14) we stay just in the point $\mathbf{I}(i, j)$, the center of the block $\mathcal{I}_{i,j}$, then we can compute the first order partial differences of $\mathbf{P}_{M_t, M_t}^{(i,j)}(x, y)$ using the central-difference formula for Krawtchouk polynomials (8) together with Eqs. (11). For example, for $M_t = 2$ we have

$$\Delta_x \mathbf{P}_{M_t, M_t}^{(i,j)}(2, 2) = \beta_{1,0}(i, j) - \beta_{1,2}(i, j), \quad \Delta_y \mathbf{P}_{M_t, M_t}^{(i,j)}(2, 2) = \beta_{0,1}(i, j) - \beta_{2,1}(i, j), \tag{15}$$

and for $M_t = 4$

$$\begin{aligned} \Delta_x \mathbf{P}_{M_t, M_t}^{(i,j)}(2, 2) &= \beta_{1,0}(i, j) - \beta_{1,2}(i, j) + \frac{3}{2} (\beta_{3,2}(i, j) - \beta_{3,0}(i, j)), \\ \Delta_y \mathbf{P}_{M_t, M_t}^{(i,j)}(2, 2) &= \beta_{0,1}(i, j) - \beta_{2,1}(i, j) + \frac{3}{2} (\beta_{2,3}(i, j) - \beta_{0,3}(i, j)). \end{aligned} \tag{16}$$

From (15) and (16), you can see that for the computation of \mathcal{P}_x and \mathcal{P}_y it is not necessary to compute all the matrices $\mathcal{B}_{n,m}$. In fact, by (16) we have that the matrices \mathcal{P}_x and \mathcal{P}_y , of the partial derivatives with respect to x or y are respectively:

$$\mathcal{P}_x = \mathcal{B}_{1,0} - \mathcal{B}_{1,2} + \frac{3}{2} (\mathcal{B}_{3,2} - \mathcal{B}_{3,0}), \quad \mathcal{P}_y = \mathcal{B}_{0,1} - \mathcal{B}_{2,1} + \frac{3}{2} (\mathcal{B}_{2,3} - \mathcal{B}_{0,3}).$$

In order to ensure that all the image boundary pixels are analyzed, we ‘fill in’ the missing pixels within the convolution operation, by mirroring the values that are inside the limits of the image \mathcal{I} across the array border.

5. Edge detection algorithm based on Krawtchouk polynomials

The proposed edge detection algorithm is based on the results of the previous sections and is described as follows:

1. Compute the matrix of gradient magnitude.

Once we obtain the matrices \mathcal{P}_x and \mathcal{P}_y , we compute in each point (i, j) the modulus of the gradient $\mathbf{G}(i, j)$ (edge strength).

$$\mathbf{G}(i, j) = \sqrt{\mathcal{P}_x^2(i, j) + \mathcal{P}_y^2(i, j)}.$$

2. Find the first threshold and the strong edge points.

We compute the first level of adaptive threshold by:

$$\tau_{h_1} = \text{mean}(\mathbf{G}(i, j)) + k \times \text{standard deviation}(\mathbf{G}(i, j)), \quad \text{where } k \in \mathbb{R}^+.$$

If $\mathbf{G}(i, j) > \tau_{h_1}$, the point (i, j) is declared as a *strong edge point*.

3. Compute the second level of threshold and the weak edge points.

Now we consider only the points (i_1, j_1) for which

$$\text{mean}(\mathbf{G}(i, j)) < \mathbf{G}(i_1, j_1) < \tau_{h_1},$$

and compute the second threshold $\tau_{h_2} < \tau_{h_1}$ by

$$\tau_{h_2} = \text{mean}(\mathbf{G}(i_1, j_1)) + k \times \text{standard deviation}(\mathbf{G}(i_1, j_1)).$$

If $\mathbf{G}(i_1, j_1) > \tau_{h_2}$, the point (i, j) is declared as a *weak edge point*.

4. Declaration of edge points.

4.1. Each strong edge point is considered an edge point.

4.2. A weak edge point is considered an edge point if at least some of its eight neighboring pixels is a strong edge point.

- 5.- Apply Morphological operations.

The matrix E_{h_2} of edge points obtained by the proposed scheme, is a matrix in which in general the edge points tend to be thick and non-continuous. Then in order to avoid these effects, it is necessary to apply morphological operations

Table 1
Error measures for the peppers image.

Measurement	ϕ^*	χ^{2*}	$F_{0.25}^*$	$F_{0.5}^*$	$F_{0.75}^*$
$EM(E, E_S)$	0.3639	0.5865	0.3536	0.3484	0.3432
$EM(E, E_C)$	0.4167	0.7317	0.4408	0.4714	0.4988

Table 2
Error measures for the depth map image.

Measurement	ϕ^*	χ^{2*}	$F_{0.25}^*$	$F_{0.5}^*$	$F_{0.75}^*$
$EM(E, E_S)$	0.1493	0.3616	0.1742	0.2002	0.2246
$EM(E, E_C)$	0.2046	0.3987	0.2124	0.2222	0.2318

[4, Chapter 14], which can be defined as combination of the two basics operations dilation and erosion [14]. Hence the final edge image E is obtained by performing in the first place the thinning operation and finally the linked operation.

6. Experimental results and conclusions

6.1. Edge quality evaluation

In order to obtain a quantitative approach measure of the edge detection method proposed, we use the statistical error measures considered in [15], where the pixels in the candidate edge image are denoted by: True Positive (TP), False Positive (FP), True Negative (TN) and False Negative (FN). Using this classification, we define the measures of the quality of an edge image: $\phi(E, E_q)$, $\chi^2(E, E_q)$ and $F_\delta(E, E_q)$ as in [15, (11)–(13)], respectively, where E_q is the true edge image. Finally to measure the errors in a edge image we use the following numbers:

$$\phi^*(E, E_q) = 1 - \phi(E, E_q),$$

$$\chi^{2*}(E, E_q) = 1 - \chi^2(E, E_q),$$

$$F_\delta^*(E, E_q) = 1 - F_\delta(E, E_q), \quad \text{where } \delta \in [0, 1].$$

To compare, we take as a true edge image E_S and E_C which are the edge images given by the Sobel (see [13, Example 15.28]) and Canny methods (see [13, Section 16.4.3]). The result for the peppers image and depth map are displayed in Tables 1 and 2, where $EM(E, E_q)$ denotes the error measure between the image edge proposed E and $E_q = E_S$ (or $E_q = E_C$).

6.2. Conclusion

The proposed algorithm has the following characteristics,

- The approximation of the partial differences (derivatives) is made with a linear combination of bivariate Krawtchouk polynomials, which are orthogonal with respect to the inner product (10), which involved the product of binomial distributions (4). Therefore, it is not necessary to smooth the image with a 2-D Gaussian filter before numerical differentiation, in order to regularize the ill-posed nature of differentiation and therefore improve the edge localization. This is a well known procedure as pointed out in [16] and used in [17].
- In [18,19] the authors describe edge detection procedures based on Chebyshev polynomials with use of a unique threshold for the whole image. Here, we propose an algorithm that uses two-level adaptive thresholds, that reduce the presence of false positive and false negative edge pixel.
- As consequence, a gradient operator of size 5×5 produces a better localized edge pixel, because the edges tend to be thicker as the size of the block $l_{i,j}$ increases [19,4].
- To avoid the thicker effect and improve the final result in our edge finder, we further apply morphological operations (close, erode and thin) to the edge image obtained after the second processing step of the proposed algorithm. As pointed out in recent work [14], this contributes to increase the quality of the edges.

Images taken from two quite different fields of application were used to demonstrate the effectiveness of the proposed algorithm: (i) natural images used for object detection, surveillance, etc.; (ii) depth maps currently used in 3D video multimedia services and applications (e.g., depth-plus-video format [20]). The results show that the proposed algorithm is able to detect the edges of different types of images. Both the contours of overlapped objects and identification of foreground objects in depth maps are obtained with quite good accuracy, as shown in Figs. 1, 2 and Tables 1, 2.

Acknowledgments

The authors dedicate this work to the memory of their friend Pablo González Vera. First and second authors work was partially supported by Ministerio de Economía y Competitividad of Spain, under grant MTM2012-36372-C03-01.



Fig. 1. Edge detection on peppers image.

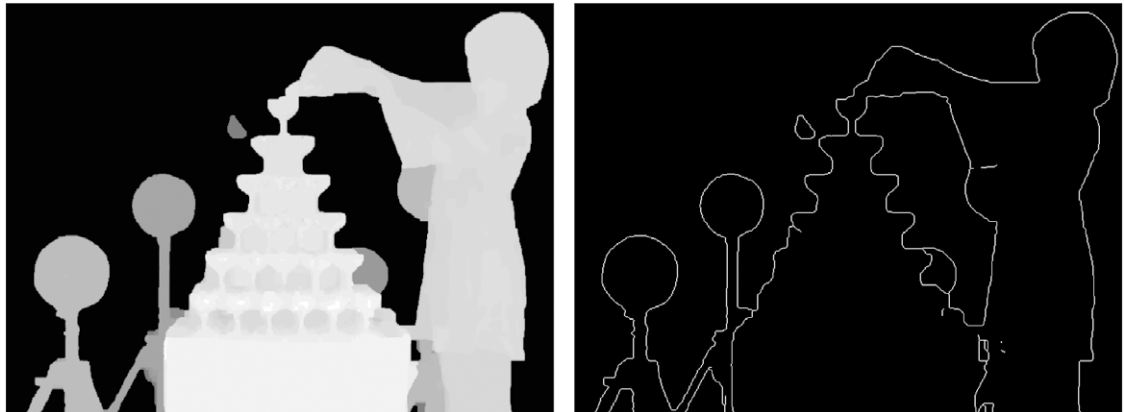


Fig. 2. Edge detection on depth map image.

References

- [1] D.J. Withey, W. Pedrycz, Z.J. Koles, Dynamic edge tracing: boundary identification in medical images, *Comput. Vis. Image Underst.* 113 (10) (2009) 1039–1052.
- [2] Y. Niu, X. Wu, G. Shi, X. Wang, Edge-based perceptual image coding, *IEEE Trans. Image Process.* 21 (2012) 1899–1910.
- [3] G. Papari, N. Petkov, Edge and line oriented contour detection: state of the art, *Image Vis. Comput.* 29 (2–3) (2011) 73–103.
- [4] W.K. Pratt, *Digital Image Processing*, John Wiley & Sons, NY, 2001.
- [5] C. Solomon, T. Breckon, *Fundamentals of Digital Image Processing. A Practical Approach with Examples in MATLAB*, Wiley–Blackwell, Oxford, 2011.
- [6] T.S. Chihara, *An Introduction to Orthogonal Polynomials*, Gordon and Breach, NY, 1978.
- [7] G. Szegő, *Orthogonal Polynomials*, in: *Amer. Math. Soc. Colloq. Publ.*, vol. 23, Providence, RI, 1975.
- [8] J. Baik, T. Kriecherbauer, K.T.-R. McLaughlin, P.D. Miller, *Discrete Orthogonal Polynomials: Asymptotics and Applications*, Princeton Univ. Press, Princeton, NJ, 2007.
- [9] A.F. Nikiforov, S.K. Suslov, V.B. Uvarov, *Classical Orthogonal Polynomials of a Discrete Variable*, Springer-Verlag, NY, 1991.
- [10] R. Beals, R. Wong, *Special Functions*, Cambridge Univ. Press, Cambridge, 2010.
- [11] J.H. Mathews, K.K. Fink, *Numerical Methods Using MATLAB*, Prentice-Hall Inc., Upper Saddle River, NJ, 1999.
- [12] J.R. Rice, *The Approximation of Functions, Vol. 2: Nonlinear and Multivariate Theory*, Addison-Wesley Publ. Co., Reading, Mass., 1969.
- [13] S.G. Hoggar, *Mathematics of Digital Images*, Cambridge Univ. Press, Cambridge, 2006.
- [14] R. Krishnamoorthi, S. Sathiyadevi, Image retrieval using edge based shape similarity with multiresolution enhanced orthogonal polynomials model, *Digit. Signal Process.* 23 (2013) 555–568.
- [15] C. Lopez-Molina, B. De Baets, H. Bustince, Quantitative error measures for edge detection, *Pattern Recognit.* 46 (4) (2013) 1125–1139.
- [16] J.V. Torre, T.A. Poggio, On edge detection, *IEEE Trans. Pattern Anal. Mach. Intell.* PAMI-8 (1986) 147–163.
- [17] C. Lopez-Molina, B. De Baets, H. Bustince, J. Sanz, E. Barrenechea, Multiscale edge detection based on Gaussian smoothing and edge tracking, *Knowl.-Based Syst.* 44 (0) (2013) 101–111.
- [18] P. Bhattacharyya, L. Ganesan, An orthogonal polynomials based frame work for edge detection in 2D monochrome images, *Pattern Recognit. Lett.* 18 (1997) 319–333.
- [19] R.M. Haralick, Digital step edges from zero crossing of second directional derivatives, *IEEE Trans. Pattern Anal. Mach. Intell.* 6 (1984) 58–68.
- [20] L. Onural, *3D Video Technologies: An Overview of Research Trends*, SPIE Press, Washington, 2011.